Journal of Biomedical Optics 9(2), 372–384 (March/April 2004)

Raman spectroscopic analysis of phase-transformation and stress patterns in zirconia hip joints

Giuseppe Pezzotti
Alessandro A. Porporati
Kyoto Institute of Technology
Ceramic Physics Laboratory &
Research Institute for Nanoscience, RIN
Sakyo-Ku, Matsugasaki
606-8585 Kyoto, Japan
E-mail: pezzotti@ipc.kit.ac.jp

Abstract. Confocal Raman piezo-spectroscopy has been used for the quantitative assessments of phase transformation and residual stresses in zirconia made artificial hip joints. This work can be considered to be a first step towards the development of a fully quantitative technique for the spectroscopic characterization of zirconia femoral heads and other zirconia parts for biomedical applications. After establishing reliable calibration procedures, Raman microprobe spectroscopy could be extended to provide quantitative assessments of zirconia metastability and microscopic stress fields along the *z* axis perpendicular to the joint surface. For the first time, we have directly visualized patterns of phase-transformation and related residual stresses on the very surface and along the subsurface of both *in vitro* tested and retrieved hip implants. These spectroscopic assessments may open a completely new perspective in understanding the micromechanical wear behavior of zirconia ceramics in biological environment and in developing new zirconia-based biomaterials with superior stability characteristics.
[DOI: 10.1117/1.1647547]

Keywords: confocal Raman spectroscopy; zirconia; artificial hip joint; phase transformation; residual stress.

Paper 03061 received May 8, 2003; revised manuscript received Jul. 31, 2003; accepted for publication Aug. 14, 2003.

1 Introduction

Raman piezo-spectroscopy using laser microprobes is becoming a more widely used technique to assess microscopic stress distributions in solids, particularly in biomedical devices.[1–3] Typically, the diameter of the focused laser beam is 1 μm, but the penetration depth may vary from tens of nanometers to several millimeters, depending upon the transparency of the investigated material. Each point within the probed volume scatters light with a Raman wave number characteristic of the local stress experienced by the solid at that point.[4] The piezo-spectroscopic interpretation of the cumulative spectrum, resulting from both distributions of light intensity and wave number shift in the probed volume, may be rather complicated and theoretical methods have been proposed for calculating theoretically the Raman spectra using stress fields derived from finite element modeling.[5] In this context, the availability of a confocal optical unit in the Raman microprobe device may offer an alternative approach to the theoretical one and enable one to perform, after appropriate calibration, a spectral deconvolution using *z* axis (i.e., the axis perpendicular to the specimen surface) displacements with relatively high spatial resolution. The micrometer spatial resolution that is nominally available for stress measurements both on the specimen surface and along the *z* axis may challenge the confocal technique being applied to quantitatively assess three-dimensional stress distributions, which vary rapidly and significantly within ever-smaller material volumes.

Address all correspondence to Dr. Giuseppe Pezzotti. Tel: 81-75-724-7568; Fax: 81-75-724-7568; E-mail: pezzotti@ipc.ki.ac.jp

Surface deterioration upon wear of *in vitro* tested or retrieved zirconia ceramic femoral heads after total hip arthroplasty is a typical biomedical item, which can be studied on a microscopic level by means of Raman spectroscopic techniques.[6–8] Two kinds of quantitative information can be achieved: (i) tetragonal-to-monoclinic phase transformation maps can be collected with a micrometer spatial resolution on selected areas of the femoral head; and, (ii) the associated residual stresses stored within the tetragonal phase can also be mapped. In previous studies,[5,7] a clear correlation was found between the degree of phase transformation and the residual stress magnitude, which is in turn related to the complex, environmentally assisted wear interactions between the femoral head and its holding acetabular cup. However, in those studies no characterization along the *z* axis was attempted; the laser microprobe, focused on the specimen surface, reached unknown depths in the zirconia subsurface, which were presumably between one and two orders of magnitude greater than the laser spot diameter. It should be noted that in wear-related phenomena both phase-transformation and stress fields are maximized on the head surface and vary rapidly with position along the *z* axis. Therefore, the approximations involved in using a subsurface penetrating laser probe can be significant and lead to underestimation of phase-transformation fractions and related residual stresses as well. In this paper, we propose a set of calibration assessments aimed to establish the quantitative use of the confocal technique in zirconia bioceramics. We have found that, in some circumstances, the interpretation of the Raman spectrum of

1083-3668/2004/$15.00 © 2004 SPIE

zirconia, in the presence of overlapping phases, is not straightforward. However, we show here an assessment of the piezo-spectroscopic behavior of all zirconia bands and locate, with the aid of confocal spectroscopy, those bands which allow reliable quantitative characterizations of transformation and stress on the specimen surface. The principles are relevant to understand surface deterioration phenomena in *in vitro* tested and retrieved zirconia femoral heads, and in other zirconia components whose performance may significantly degrade due to phase metastability in humid environment.

2 Materials and Methods

A new femoral head (28 mm in diameter), made of polycrystalline ZrO_2 containing 3 mol % Y_2O_3 for stabilization (3Y-TZP), was provided by St. Gobain Desmarquest, Evreux, France. This head appeared to be mechanically drilled after sintering to obtain a cylindrical hole for fixture. After drilling, the internal surface of the hole was left unpolished, thus, showing significant roughness. The head was kept for 5 h in a climate test chamber operating in vapor (2 atm) at 394 K, which roughly correspond to 1 y in the human body.

Another hip implant was a 26 mm zirconia ball (3Y-TZP) retrieved from a 49-year-old male. Ethylene gas was used as sterilization medium before implantation, therefore no deterioration phenomenon is to be ascribed to pre-surgery manipulation. The ball was implanted first in 1994 and pain and instability developed in 1997 (follow-up=3 years less 2 months) without any obvious cause. Polyethylene ring dislodging was noted by x-ray analysis. This case experienced a strong impingement of cup against the metal neck of femoral stem. Remarkable amounts of tetragonal-to-monoclinic phase transformation were observed in some regions in previous studies. A clinical analysis of the retrieved case is beyond the goal of the present investigation (more details can be found in Refs. 7 and 9); here, we mainly focus on establishing the appropriate spectroscopic procedures for quantitatively analyzing the retrieved hip implant.

Zirconia specimens for piezo-spectroscopic calibrations were laboratory made 3Y-TZP and pure monoclinic zirconia sintered bodies. The 3Y-TZP specimens were sintered from the same starting powder used for preparing the femoral heads (grade TZ-3Y, Tosoh, Tokyo, Japan) and, similar to the implants, showed a submicrometer grain size. Pure monoclinic zirconia powder was also from a commercially available grade (grade TZ-0, Tosoh, Tokyo, Japan).

Raman spectra were collected with a triple monochromator spectrometer (T-64000, ISA Jovin-Ivon/Horiba Group, Tokyo, Japan) equipped with a charge coupled detector [high-resolution charge coupled device (CCD) camera]. In mapping of phase fractions and stresses, the required laser power on the zirconia surface was typically about 400 mW at the laser head and a suitable excitation frequency was the blue line at 488 nm of an Ar-ion laser. The spectrum integration time was typically 4 s, with averaging the recorded spectra over three successive measurements. A preliminary calibration was performed with recording the dependence of the zirconia spectrum (in a tetragonal/monoclinic mixed region) on the laser power and integration time. No change was noticed in the relative intensity of bands arising from different polymorphs up to 600 mW and a few minutes of accumulation time, thus confirming that sample heating does not perturb the phase composition for the selected measurement conditions.

All the spectra were recorded at room temperature. The optical microscope was connected to a video monitor that allowed scanning of the sample to locate and observe the desired positions on the surface. The Raman peak positions were obtained by fitting the CCD raw data to mixed Gaussian/Lorentzian curves with commercially available software. Zirconia specimens were placed on a mapping device (lateral resolution of 0.1 μm), which was connected to a personal computer to drive highly precise displacements (along both x and y axes) on the specimen surface. An auto-focus device was adopted throughout automatic mapping experiments.

In confocal Raman experiments, the laser light from the probe head was focused to a diffraction-limited spot on the zirconia sample surface by the microscope objective. Raman signal was refocused onto a small confocal aperture that acted as a spatial filter, passing the Raman signal excited at the beam waist, but eliminating Raman signals produced at other points above and below the beam waist. The filtered Raman signal then returned to the spectrometer (via the probe head) where it was dispersed on to the CCD camera to produce a spectrum. In practice, a pinhole aperture was placed in the optical train of the microspectrometer and used to regulate the rejection of out-of-focus light. It should be noted that, conventionally, confocal spectroscopy is done with a fixed aperture to limit the detection of photons collected outside of some specific z axis distance from the beam waist of the focused spot. Then spectra are acquired which are a function of z by changing the focus of the microscope from surface to subsurface. In this paper, we used a different approach where the focus is fixed in the z direction and the pinhole aperture size is varied. This will give an increasing integration along the z axis as the aperture is opened, but no effect will arise due to the refractive index of zirconia, thus avoiding a difficult assessment of local refractive index in partly transformed areas consisting of different polymorphs. Confocal Raman microscopy was used to probe selected xyz locations in the zirconia sample, with micron (lateral) spatial resolution. Data slices were built up by xy scanning the sample, and three-dimensional data sets were produced by sequentially acquiring a set of xy slices at different z depths.

In assessing the piezo-spectroscopic behavior of zirconia Raman spectra, a ceramic bar was mounted on a four-point bending jig and placed under the optical microscope. Load was applied and the whole jig was moved under the optical microprobe to record spectra every 50 μm along the specimen thickness. The applied load was converted to stress using the standard four-point bending elastic beam equation and the recorded Raman shifts plotted as a function of elastic stress. The slope of stress/shift plots, Π_u, was precisely recorded to an extent and used throughout stress assessments of unknown residual stress fields. As far as elastic stress fields are concerned, applied stresses recorded along a line perpendicular to the long axis of the specimen bar (i.e., along the thickness at the center of the bar) can be regarded as uniaxial and linearly changing from compression to tension (at the sides of small and large span of the four-point bending bar configuration, respectively).

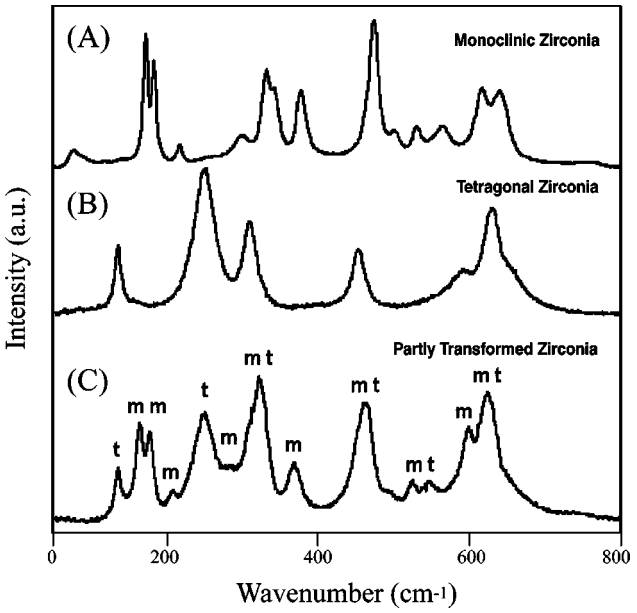

Fig. 1 Typical Raman spectra of monoclinic and tetragonal zirconia collected from their monolithic bodies [(A) and (B), respectively]. In (C), a Raman spectrum collected from an area, which underwent partial tetragonal-to-monoclinic transformation. Tetragonal and monoclinic bands are located by *t* and *m*, respectively.

3 Results and Discussion

3.1 *Zirconia Phases and their Quantitative Determination from Raman Spectra*

Zirconia ceramic can be found in nature as three low-pressure structural polymorphs. The zirconia system passes from a monoclinic ground state to a tetragonal phase, and then eventually to a cubic phase, with increasing temperature. The monoclinic phase space group (C_{2h}^5 or $P2_{1/c}$) is thermodynamically stable below 1400 K. Around 1400 K, a transition occurs to the tetragonal structure (space group D_{4h}^{15} or $P4_2/nmc$), which is a slightly distorted version of the cubic structure and is stable up to 2570 K. Finally, the cubic phase (space group O^5h or $Fm3m$) is thermodynamically stable between 2570 K and the zirconia melting temperature at 2980 K. In the monoclinic phase there are two nonequivalent oxygen sites with coordination numbers of 3 (O_1) and 4 (O_2), while all the Zr atoms are equivalent and have a coordination of 7.[10,11] Phase transformation and low-temperature metastability are the most relevant problem in zirconia materials for biomedical applications. Low-temperature aging significantly affects both phase structure and mechanical properties because it involves tetragonal-to-monoclinic transformation. The phase transformation can be relevantly enhanced by water or water vapor.[12]

According to group theory,[10] the Raman spectrum of zirconia materials at 300 K should consist of 18 peaks, however several of these peaks are not observed experimentally. Of major interest in biomedical applications are the tetragonal, the monoclinic phases with their overlapping spectra. Figure 1 shows typical Raman spectra of zirconia which were collected in a pure monoclinic specimen (A), pure tetragonal specimen (B), and in a partly transformed tetragonal/monoclinic transformation zone (C) (excitation frequency of 488 nm; laser power of 400 mW and integration time of 15 s). As seen, tetragonal and monoclinic bands largely overlap, but a relatively strong and sharp band exists at 142 cm^{-1} only for the tetragonal phase, in addition to the more intense (but broader) tetragonal band located at 256 cm^{-1}. Two intense bands are also observed for the tetragonal phase at around 316 and 460 cm^{-1}, but partial transformation to monoclinic phase superimpose to these latter tetragonal bands two monoclinic bands of comparable intensity. The monoclinic phase also shows a relatively sharp doublet at 178 and 190 cm^{-1}, which is not overlapped with any tetragonal bands, in addition to a weaker (and slightly broader) band located at 384 cm^{-1}. The monoclinic content of zirconia phase, V_m, contained into a partly transformed zone, can be quantitatively evaluated from the relative intensities of selected (i.e., nonoverlapping) Raman bands, which belong to the tetragonal phase (145 and 260 cm^{-1} bands) and to the monoclinic phase (178 and 189 cm^{-1} bands). The following formula can be used, which was first proposed by Clarke and Adar[13] for such structural assessments:

$$V_m = (I_m^{178} + I_m^{189})/0.97(I_t^{145} + I_t^{260}) + I_m^{178} + I_m^{189}, \qquad (1)$$

where I represents the intensity of the band identified by the apex, and the subscripts m and t identify the monoclinic and tetragonal polymorphs, respectively. The technique was accurate to about 0.2 vol %, as determined by the limit of detectability of the two monoclinic peaks.

3.2 *Stress Dependence of the Raman Spectra of Zirconia*

The Raman bands of optical phonons in crystals shift under stress. The amount of band shift due to stress is determined by the phonon deformation potential, a material property.[5] The presence of lattice stress lifts the degeneracy of the optical phonon modes in zirconia and changes their wave numbers. The new wave numbers are related to the lattice stress field, but the relationships are complicated because the observed spectrum depends on the crystal structure, the polarization and propagation vectors of the incident and scattered light with respect to the crystal axes, and the geometrical state of the local stress field.[4,5] In addition, in polycrystalline materials the crystal structure is not resolvable because many grains are present with different orientations within the probed volume. In this case, only a phenomenological approach can be adopted, according to which the stress dependence is evaluated experimentally for a given stress field (i.e., an uniaxial field for the calibration in the present investigation). Piezo-spectroscopic calibration plots for the 142 cm^{-1} band of tetragonal phase and the 384 cm^{-1} band of monoclinic phase under uniaxial stress are shown in Figs. 2(A) and 2(B), respectively. The stress dependence of all the peaks of zirconia phases is linear below a certain stress level and the slope of these plots (obtained by least-square fitting of the experimental data) is defined as the respective piezo-spectroscopic coefficient, Π_u. A complete list of the piezo-spectroscopic coefficients of both tetragonal and monoclinic bands of zirconia is given in Table 1, in which unstressed (reference) wave numbers and the respective standard error are also shown. These stress dependences have been determined on dense monolithic

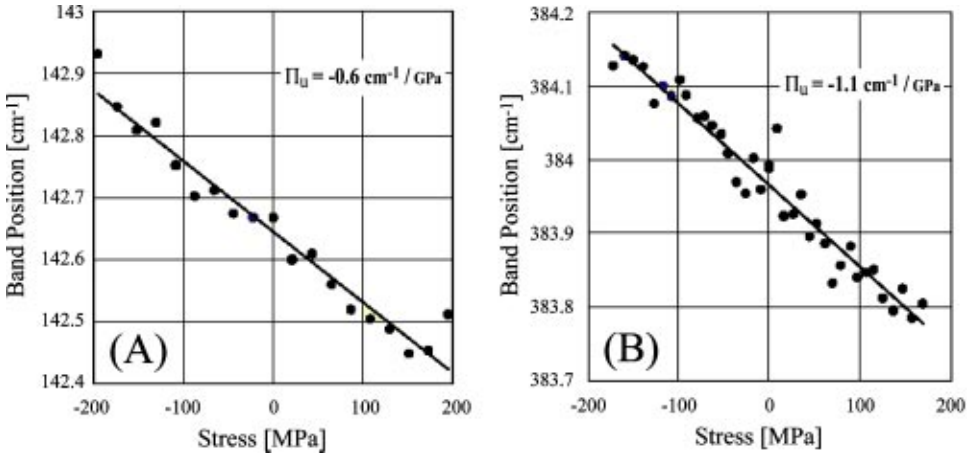

Fig. 2 Stress calibration lines collected on the 142 cm^{-1} band of the tetragonal phase (A) and on the 384 cm^{-1} band of the monoclinic phase (B).

bodies consisting of either monoclinic or tetragonal phase. From the standard deviations of piezo-spectroscopic plots (cf. Table I), it can be found that the highest reliability band for stress assessments in a (monolithic) tetragonal zirconia polycrystal is located at 460 cm^{-1}, followed by the 316 and 142 cm^{-1} bands. The 480 cm^{-1} band, which partly overlaps the most reliable band of the tetragonal phase, and all the other bands of the monoclinic phase are less reliable in stress assessment than the tetragonal bands. An exception is the 384 cm^{-1} band, whose standard deviation was comparable with that of the 316 cm^{-1} tetragonal band. However, it should be noted that the monoclinic band with the highest stress sensitivity (i.e., the highest Π_u value) was also a band of low reliability. This may arise from a high dependence of the zero-stress wave number of this band on the crystallographic orientation of individual crystallites in the polycrystal.

In assessing residual stresses related to phase transformation, we assumed a hydrostatic stress field in a homogeneous and isotropic body. Accordingly, a three-dimensional piezo-spectroscopic coefficient, $\Pi_h = 3\Pi_u$, has been used throughout the stress assessments. Finally, it should be noted that, in the bending configuration used in the present piezo-spectroscopic calibrations, the stress field is independent of the z axis perpendicular to the stress surface.

3.3 *Assessment of In-Depth Raman Probe Response*

In Raman spectroscopic assessments, the precise knowledge of shape and dimension of the laser probe in the specimen is of fundamental importance. In addition, with the availability of a confocal probe device, the penetration depth of the probe within the specimen can be controlled to an extent and data collected as a function of an abscissa taken along the z axis perpendicular to the specimen surface. However, an appropriate calibration should be pursued to quantitatively assess the penetration depth of the laser probe in the subsurface. In this study, we used a wedge-shaped specimen, whose geometry is shown in Fig. 3, to determine the laser penetration depth in zirconia. An acuminate edge could be obtained with an average radius of curvature of only 1 μm, using a machining technique, which was standardized by the Kyocera Co. for the edge of a ceramic knife. The wedge-shaped specimen, which was made from a monolithic piece of (tetragonal) polycrystalline zirconia, was irradiated by a 488 nm laser emitted with a power of 200 mW. The optical (lateral) resolution was 1 μm, and the intensity of all the spectroscopic bands of zirconia was recorded as a function of the thickness of the material in various confocal configurations. A typical plot of spectral intensities as a function of length, X, along the wedge-shaped specimen, is shown in Fig. 4 for the 460 cm^{-1} band of tetragonal zirconia. The maximum penetration depth, Z, to which the intensity of the collected Raman spectrum is contributed, can be obtained from this plot by simple geometrical considerations and by monitoring the minimum thickness value, above which the band intensity saturates to a constant value. Then, an additional plot can be drawn of such a maximum depth as a function of confocal configuration parameter (Fig. 5). This latter plot represents the foundation for in-depth assessments on zirconia surfaces.

An interesting application of the confocal setup can be obtained by monitoring the morphological evolution with increasing the laser penetration depth of the overlapping zirconia bands located at 460 and 480 cm^{-1}, for the tetragonal and monoclinic phase, respectively. Spectra were collected on the retrieved zirconia ball described in Sec. 2. Figure 6 shows a sequence of spectra, taken in a selected area of the retrieved ball, in which tetragonal-to-monoclinic transformation partly occurred. Spectra are displayed as a function of depth, z, below the external surface of the ball. Volume fractions and penetration depths explicitly shown in Figs. 6(A)–6(E) were calculated according to Eq. (1) and the plot in Fig. 5, respectively. For better clarity, deconvoluted spectra composed of three bands (460 cm^{-1} tetragonal band, 480 and 508 cm^{-1} monoclinic bands) are also shown. As seen, a shallow probe configuration detects a higher amount of monoclinic phase, as confirmed by the increasingly higher intensity of the monoclinic band located at 480 cm^{-1}, as compared to the tetragonal 460 cm^{-1} band. With increasing penetration depth of the laser probe, Z, the fraction of monoclinic phase decreases because it represents an average value over the probed volume in the subsurface. For a penetration depth of 40 μm, the detected amount of monoclinic phase becomes negligible ($V_m = 1\%$) and the monoclinic band intensity is almost negligible with respect to the tetragonal one. In these circumstances, a straightforward spectroscopic examination [cf. de-

Table 1 Raman band position, relative intensity and uniaxial piezo-spectroscopic coefficient, Π_u, (i.e., the slope of a plot of band spectral shift, $\Delta\nu$, as a function of uniaxial stress, σ, as shown in Fig. 2) collected for all the bands of the tetragonal and monoclinic (monolithic) zirconia phases. The square correlation coefficient, R^2, is also shown in order to assess the reliability of the piezo-spectroscopic stress measurement. This coefficient is defined as: $R_{xy}^2/R_{xx}R_{yy}$, where R_{xx}, R_{yy} and R_{xy} are average data scatters along the x and y axes (i.e., σ and $\Delta\nu$, respectively) and the average distance of data plots from a least-square fitting line, respectively. The relative intensities have been calculated by arbitrarily assigning a value 100 to the most intense Raman band in each phase.

	Band position (cm^{-1})	Relative intensity	Π_u (cm^{-1}/GPa)	R^2
Tetragonal phase	144.68	56	−0.6	0.95
	259.57	100	1.1	0.76
	318.03	69	−1.3	0.96
	461.72	53.6	−1.4	0.98
	604.76	42.9	1.1	0.10
	635.14	78.6	−0.5	0.62
	641.21	44	−0.8	0.04
Monoclinic phase	178.29	92.9	−0.9	0.91
	189.38	76.2	−0.8	0.89
	223.07	30.9	−0.6	0.70
	304.99	35.7	−2.8	0.91
	349.32	71.4	−1.6	0.94
	383.97	59.52	−1.1	0.95
	479.49	100	−0.9	0.86
	507.88	38.1	−0.8	0.88
	536.63	40.5	−1.9	0.91
	569.95	40.5	−1.9	0.88
	622.18	61.9	−2.4	0.95
	647.23	59.5	−2.6	0.90

convoluted spectrum in Fig. 6(E)] suggests that the wave number shift of the 460 cm^{-1} tetragonal band with stress can be considered to be unaffected by the presence of the neighboring monoclinic bands. A plot can be also obtained (Fig. 7) of monoclinic volume fraction, V_m, versus the relative intensity, I_m^{480}/I_t^{460}. This plot can be expressed by the following equation:

$$V_m = 20.2(I_m^{480}/I_t^{460}), \quad (2)$$

which is valid for $5\% < V_m < 25\%$ and represents an alternative to Eq. (1), with the disadvantage of requiring a spectral deconvolution procedure, but with the advantages of being

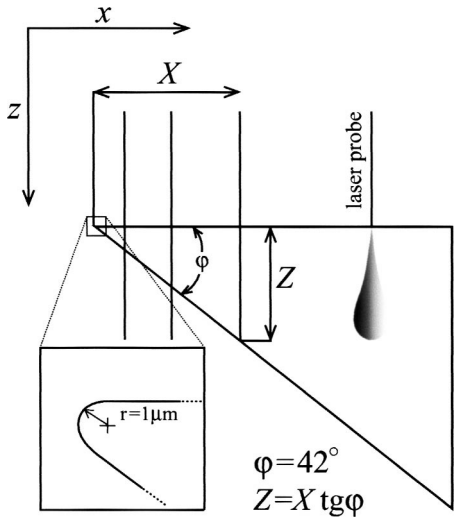

Fig. 3 Schematic of the procedure adopted for the experimental assessment of laser penetration depth in polycrystalline zirconia.

more sensitive to the presence of monoclinic fraction and of involving spectral monitoring of a narrower wavelength interval with respect to Eq. (1).

Spectroscopic data in Fig. 6 clearly suggest the need of confocal Raman assessments for properly assessing the actual transformed fraction to monoclinic phase in retrieved zirconia femoral heads. Transformation in zirconia hip joints is driven by wear and assisted by environmental factors; it proceeds from the surface towards the subsurface of the ball according to complicated patterns, and the propagation depth, function of time and wear parameters cannot be made obviously available from conventional analytical methods (e.g., x-ray or neutron diffraction analyses). A visualization of these patterns

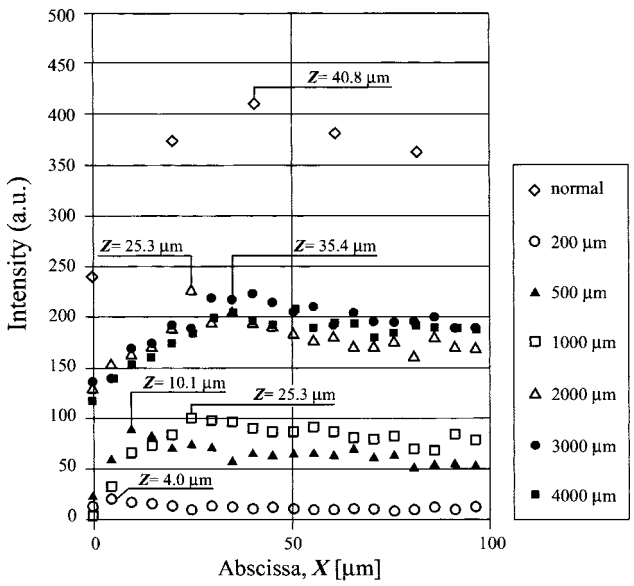

Fig. 4 Plot of the intensity of the 460 cm^{-1} band of tetragonal zirconia as a function of the length, X, along the wedge-shaped specimen shown in Fig. 3.

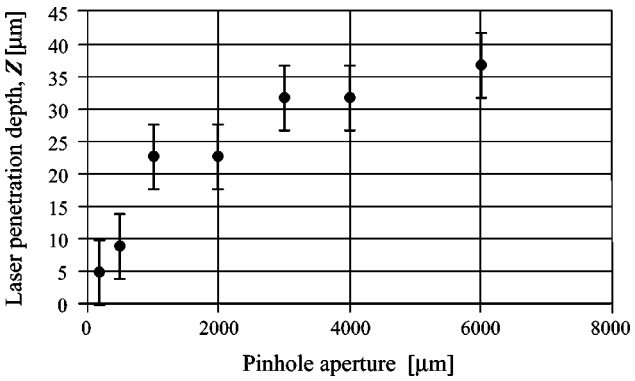

Fig. 5 Plot of the laser penetration depth, *Z*, along the zirconia subsurface as a function of the pinhole aperture in the confocal configuration of the Raman microprobe device.

(and of the residual stresses involved with them) as a function of an abscissa along the *z* axis is attempted in the next section.

3.4 *Patterns of Phase-Transformation and Residual Stress in Hip Joints*

To examine more in detail the transformation process and to study its relationship with residual stresses, two-dimensional maps ($20\times20\ \mu$m along two perpendicular *x* and *y* arbitrarily selected directions) of monoclinic volume fraction and residual stress in the tetragonal phase were collected at selected locations, in which tetragonal-to-monoclinic phase transformation partly occurred. Figure 8 shows an optical micrograph of the internal surface of the fixture hole drilled (after sintering) inside a new 3Y-TZP zirconia ball. Presumably, the ball was not annealed after drilling and the surface of the internal hole showed deep and regular roughness patterns, left on the surface by the drilling tool. After autoclaving in humid atmosphere, transformation clearly proceeded along

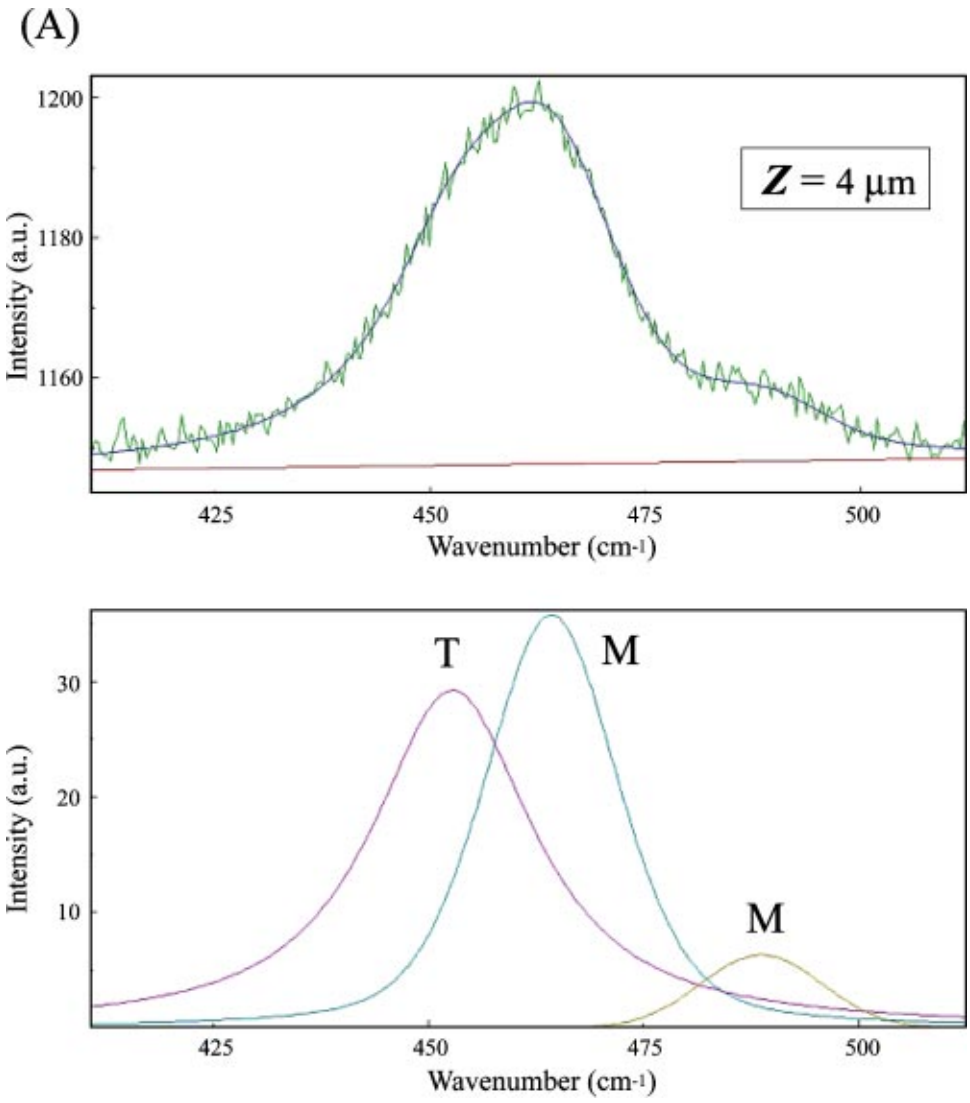

Fig. 6 Morphological evolution of overlapping zirconia bands located at 460 cm^{-1} (tetragonal band), 480 and 508 cm^{-1} (monoclinic bands) with increasing laser penetration depth, *Z*, along the subsurface of a partially transformed (retrieved) zirconia ball. The experimentally collected bands and their respective deconvolutions into three subbands are shown for each *Z* value.

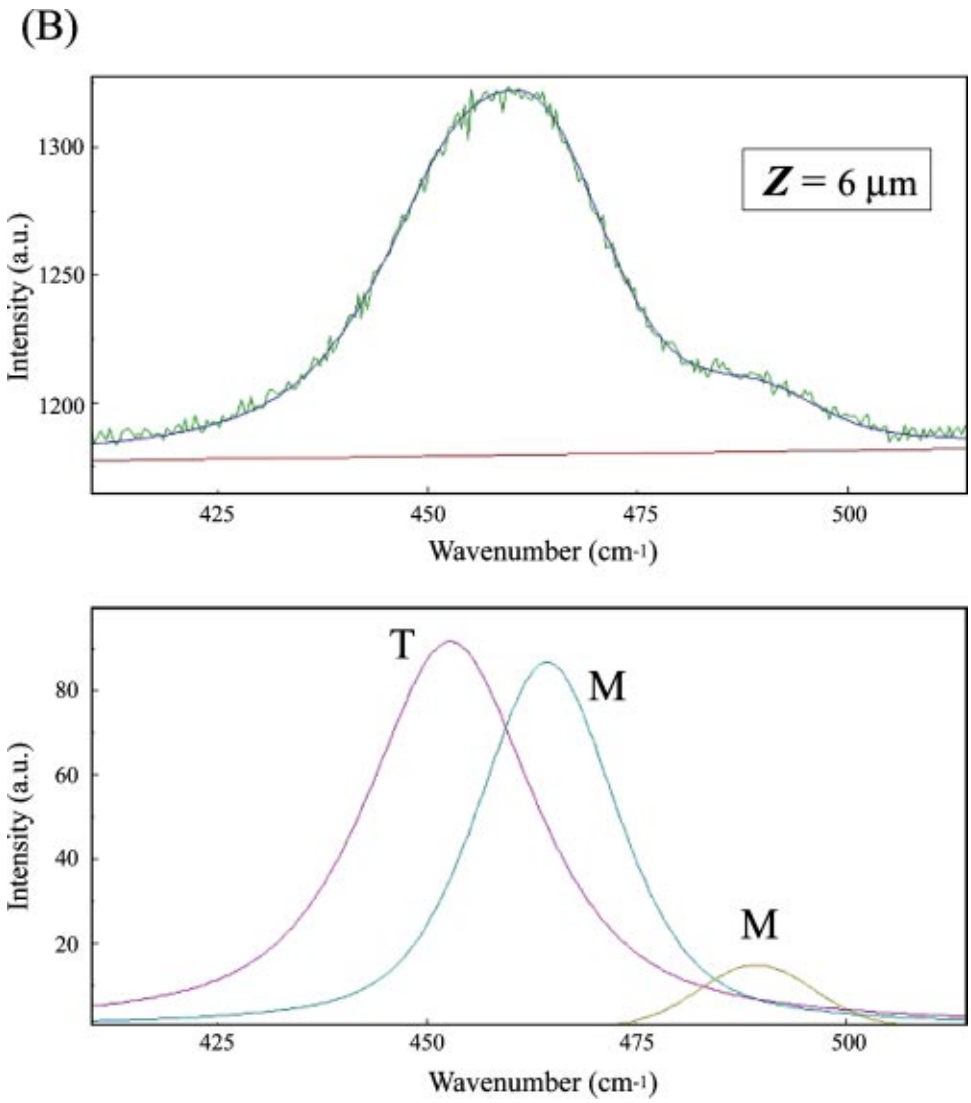

Fig. 6 (*Continued.*)

the preferential paths of surface scratches. This was proved by a confocal Raman map of monoclinic fraction, as shown in Fig. 9(A), which corresponds to the square area depicted in the optical micrograph in Fig. 8. This map was collected with a pinhole confocal aperture corresponding to a laser penetration depth of only 4 μm. The entire surface underwent partial phase transformation, with a maximum monoclinic content as high as 58% in the mechanically scratched regions. Additional phase-transformation maps [Figs. 9(B)–9(E)] were collected at the same location as a function of confocal pinhole aperture, but with higher laser penetration depths, Z. As the volume probed by laser increased (i.e., with increasing Z), the transformation map lost its correspondence to the optical micrograph, because the probe averaged the Raman signal over highly transformed area on the surface and less transformed internal volume as well. The average monoclinic fraction was 41% when probing with a penetration depth of 4 μm, but it was significantly reduced to 9% with $Z = 40$ μm. Again, it appears evident that, for a correct assessment of the transformed monoclinic fraction on the surface, it is preferable a confocal Raman probe configuration.

Surface residual stress fields in zirconia hip joints may be rather complicated because of the overlapping of several factors, including phase transformation, machining, etc. Residual stresses associated with the tetragonal-to-monoclinic phase transformation are expected to be tensile in the tetragonal phase and compressive in the monoclinic phase,[14] because the transformation occurs with significant volume expansion. However, an additional stress field of remarkable magnitude may be induced by machining procedures, as the hole drilling discussed in this report. This latter residual stress field is generally compressive in nature and its absolute value may be significantly larger than that of phase-transformation-related stresses. Figures 10(A)–10(E) show stress maps (drawn from the shift of the 460 cm^{-1} tetragonal band according to the piezo-spectroscopic coefficient listed in Table I), which were

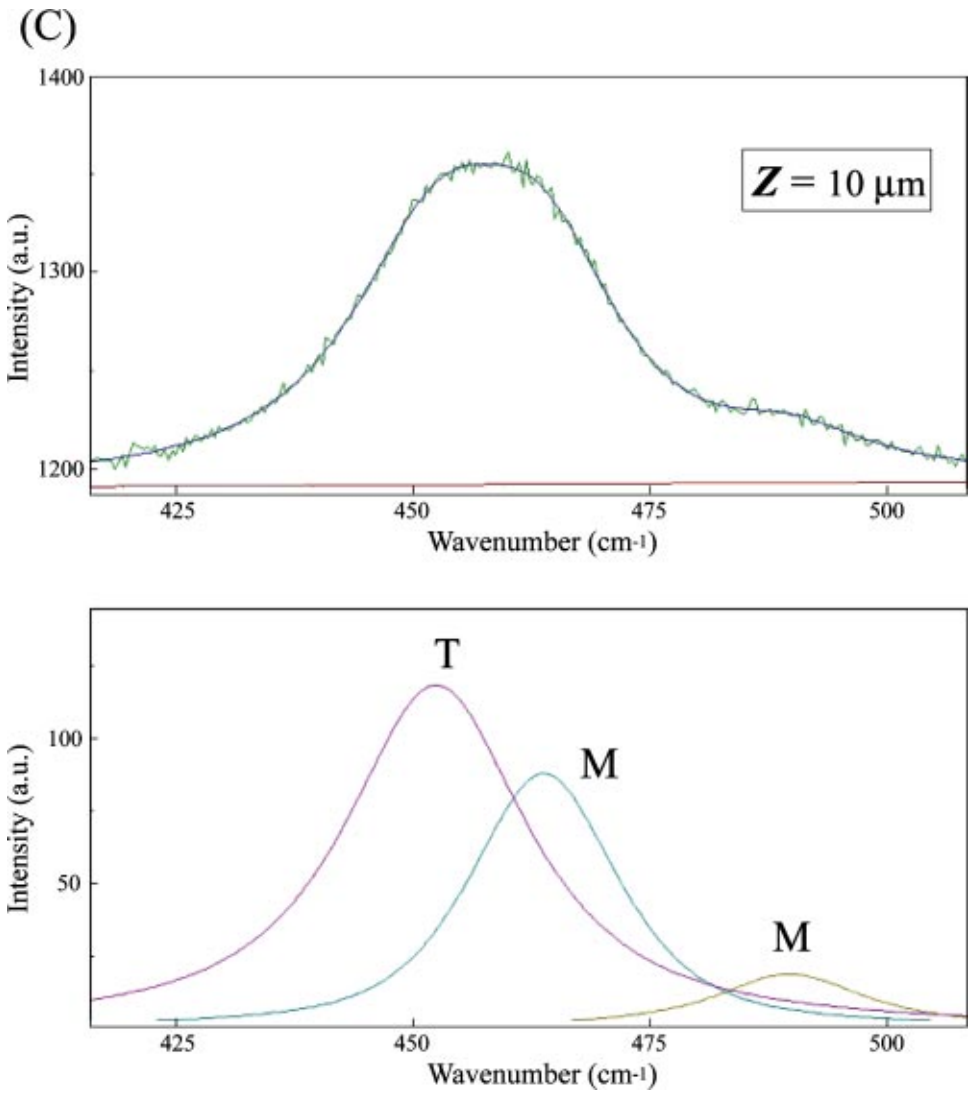

Fig. 6 (*Contined.*)

collected at the same location shown in Fig. 8. These stress maps were obtained at different Z values, which were the same as that displayed in the corresponding maps in Fig. 9. Compressive stresses were always detected on the drilled surface, independent of Z value. However, their magnitude strongly decreased with increasing Z. This experimental finding can be explained with invoking the higher magnitude of stress at the very surface as compared with the subsurface; this argument is similar to that used for explaining the trend already found for phase transformation in Fig. 9. However, in the case of stress assessments there is an additional complication, which arises from the spectroscopic trend observed in Fig. 6 for overlapping 460 and 480 cm^{-1} bands of tetragonal and monoclinic phase, respectively. From Fig. 6, we have noticed that in mixed phase areas, the above band can be considered to behave as a fully tetragonal band only for $V_m < 10\%$, which is the case of $Z = 40$ μm [Fig. 10(E)]. In other words, the correct magnitude of residual stress can be obtained in partly transformed areas, but only upon averaging over a relatively large volume (i.e., not in a confocal configuration), because of band overlapping. Higher values of residual stresses were obtained at smaller Z values but, despite the high intrinsic reliability of the 460 cm^{-1} tetragonal band for stress assessment, these values may not represent the actual residual stress magnitude because overlapping of the 480 cm^{-1} monoclinic band is not negligible.

On the other hand, in areas where transformed fractions are largely preponderant ($>60\%$), the mixed band 460/480 cm^{-1} turned to be mainly affected by its monoclinic component. Therefore, the assessment of the overall band may be reliable to a certain degree of precision for stress determination (in the monoclinic phase) under any optical configuration. Figure 11 shows phase transformation maps [(A) and (C)] and related stress maps in the monoclinic phase [(B) and (D)], as collected in a polar location of a retrieved 3Y-TZP femoral head. The maps shown in Figs. 11(A) and 11(B) were collected in a confocal configuration with a laser penetration depth of $Z = 4$ μm, while for those shown in Figs. 11(C) and 11(D) $Z = 40$ μm. The selected area was characterized by an exceptionally high degree of monoclinic transformation. Therefore, residual stresses have been piled up due to

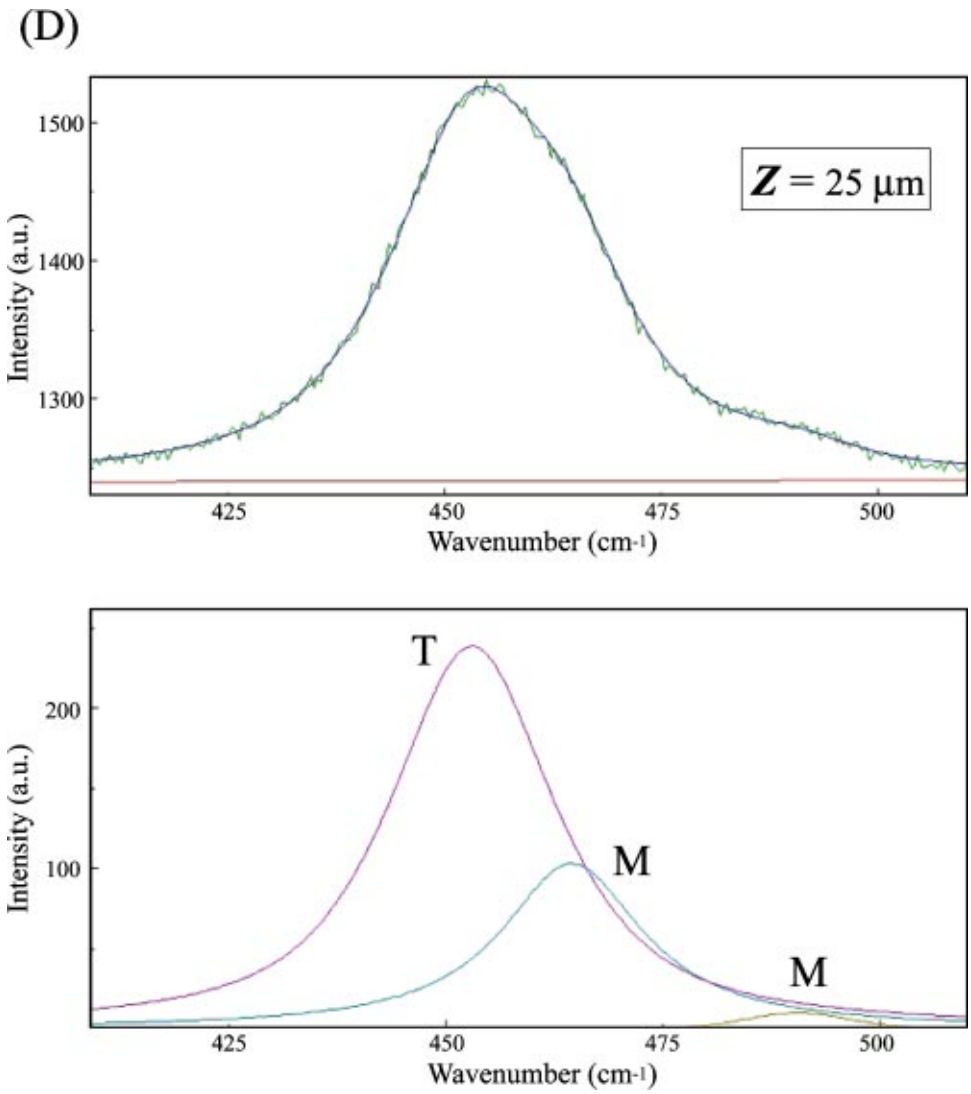

Fig. 6 (*Continued.*)

the combined effects of phase transformation and mechanical impingement/wear of the femoral head against the acetabular cup. Both effects should lead to a compressive residual stress field in the monoclinic phase, as confirmed by the Raman experiment. A very good correspondence was found between the patterns of phase transformation and those of residual stress, which we consider to be a confirmation for the validity of the present piezo-spectroscopic assessments. As expected, both monoclinic fraction and stress magnitude were higher at the ball surface, as compared to the subsurface. The confocal probe configuration was found to be extremely useful in assessing the actual magnitude of residual stresses.

4 Conclusion

Raman spectroscopic techniques have been discussed, which aim at assessing both phase-transformation and residual stress in 3Y-TZP as a material for total hip joint replacement. By means of appropriate calibrations of phase and stress dependence of selected Raman bands, microscopic phase-transformation and stress patterns could be quantitatively assessed with a typical spatial resolution of 1 μm. Microscopic residual stress fields were clearly related to the tetragonal-to-monoclinic transformation in 3Y-TZP after machining and wear both *in vitro* and *in vivo*, and this semiempirical criterion of phase/stress correspondence was adopted for addressing the actual validity of Raman spectroscopic assessments. The confocal probe configuration was calibrated for quantitatively determining the laser penetration depth, Z, in 3Y-TZP. According to this calibration, it was found that the most reliable measurement in assessing the actual fraction of transformed monoclinic phase could be obtained with $Z<4\ \mu$m. All the available Raman bands of tetragonal and monoclinic phase were calibrated with respect to their respective shifts upon application of a known uniaxial stress field. As a general trend, tetragonal bands allowed a more reliable stress assessment as compared to monoclinic bands. Among tetragonal bands, the one located at 460 cm^{-1} was highly reliable and sensitive to stress, although overlapping with the 480 cm^{-1} monoclinic band was not negligible for transformed fractions $>10\%$. For monoclinic fractions $>60\%$, the 480 cm^{-1}

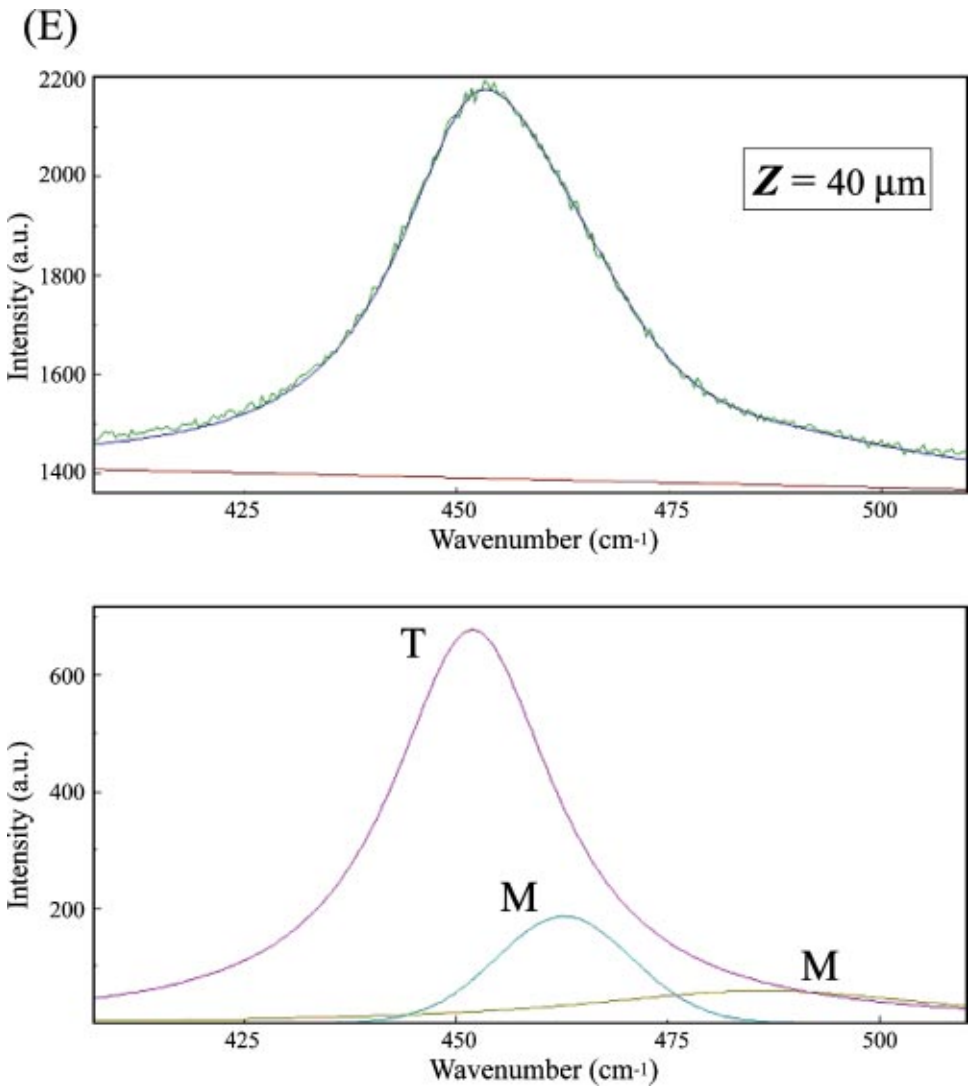

Fig. 6 (*Continued.*)

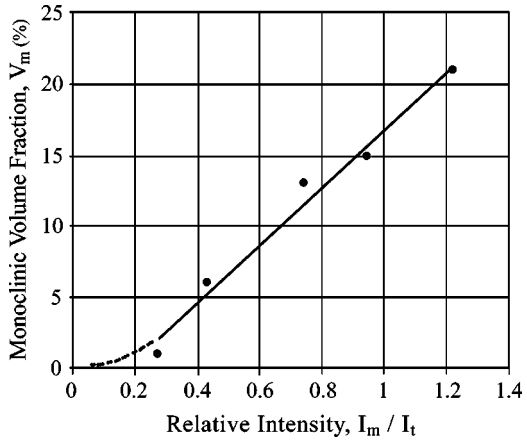

Fig. 7 Plot of monoclinic volume fraction, V_m, versus the relative intensity ratio, I_m^{480}/I_t^{460}, as obtained according to data in Fig. 6.

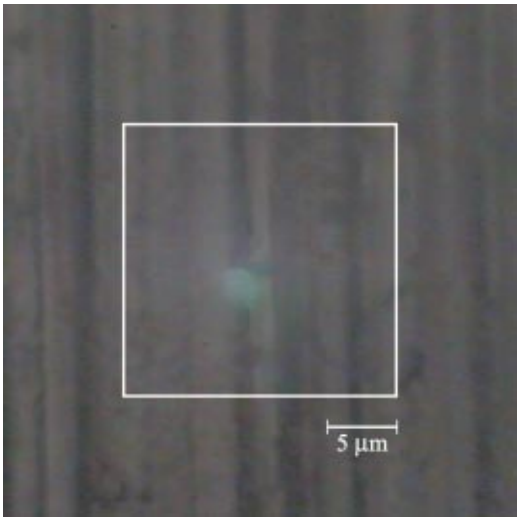

Fig. 8 Optical micrograph of the internal surface of the fixture hole drilled (after manufacturing) inside a new 3Y-TZP zirconia ball. Dark lines correspond to drilling paths.

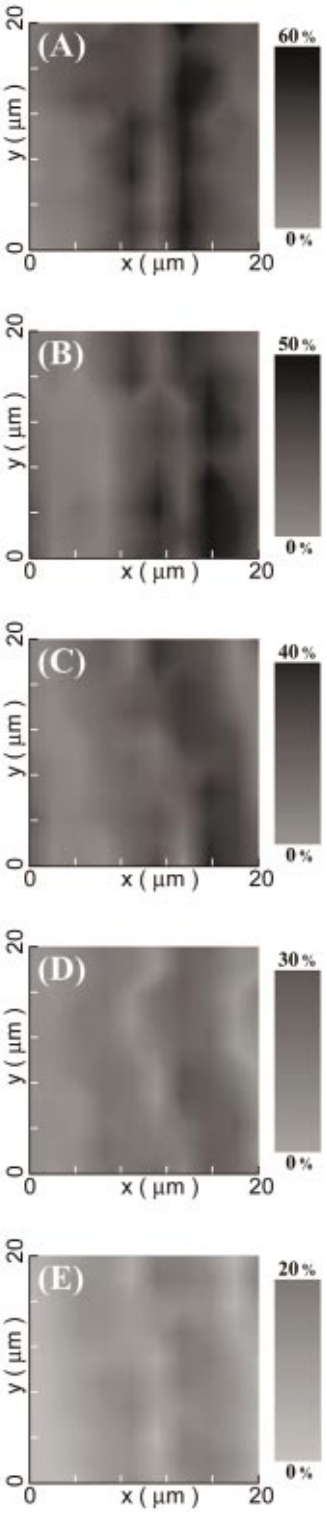

Fig. 9 Phase-transformation maps collected at the location shown in Fig. 8 as a function of laser penetration depth, Z, [(A)–(E) correspond to $Z = 4,\ 6,\ 10,\ 25,\ 40\ \mu$m, respectively].

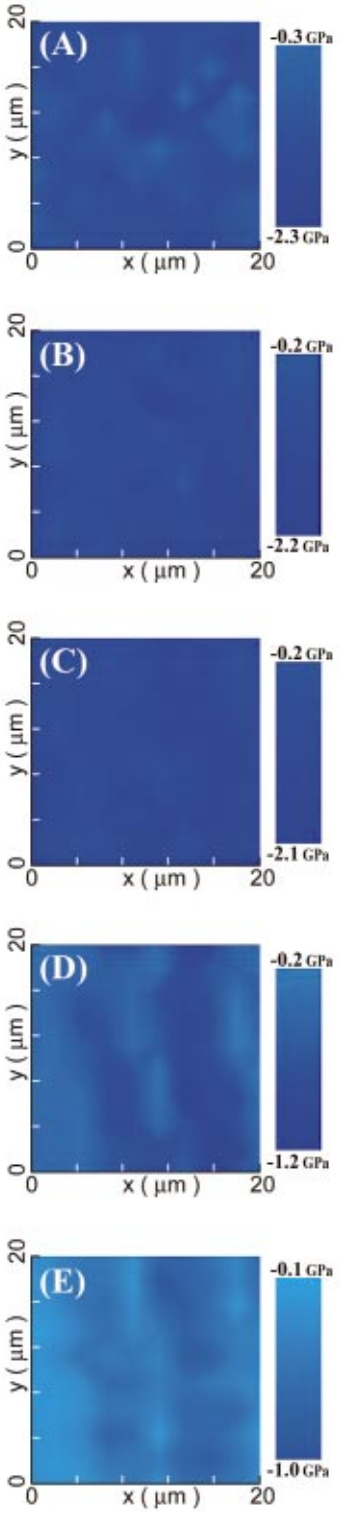

Fig. 10 Residual stress maps (from the shift of the 460 cm^{-1} tetragonal band according to the piezo-spectroscopic coefficients listed in Table I) collected at the location shown in Figs. 8 and 9 as a function of laser penetration depth, Z, [(A)–(E) correspond to $Z = 4,\ 6,\ 10,\ 25,\ 40\ \mu$m, respectively].

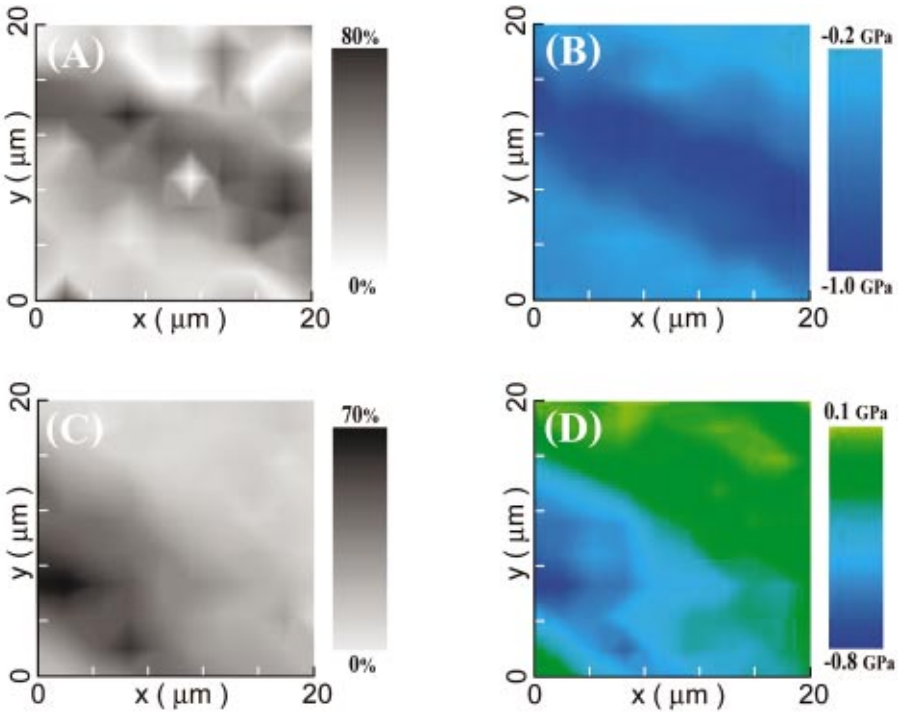

Fig. 11 Monoclinic phase-transformation maps [(A) and (C)] and related stress maps in the monoclinic phase [(B) and (D)], as collected in a polar location of retrieved femoral head. The maps in (A) and (B) were collected in a confocal configuration with a laser penetration depth of $Z = 4\ \mu$m, while for those shown in (C) and (D) $Z = 40\ \mu$m.

monoclinic band became preponderant and residual stresses in the monoclinic phase could be assessed with a good degree of approximation.

This paper demonstrates that a quantitative knowledge of phase-transformation and stress fields on a microscopic scale, achieved through Raman spectroscopy, may enable replacing the empirical optimization of biomaterials processing with more rational procedures, thus greatly enhancing the speed for the development of new materials.

Acknowledgments

The authors gratefully thank S. Sakakura for his help with the piezo-spectroscopic measurements. This work could not have been possible without the invaluable scientific contribution and continuous encouragement by Professor I. C. Clarke and Professor B. Ben-Nissan.

References

1. J. A. Timlin, A. Carden, M. D. Morris, J. F. Bonadio, C. E. Hoffler II, K. M. Kozloff, and S. A. Goldstein, ''Spatial distribution of phosphate species in mature and newly generated mammalian bone by hyperspectral Raman imaging,'' *J. Biomed. Opt.* **4**, 28–34 (1999).
2. A. Carden and M. D. Morris, ''Application of vibrational spectroscopy to the study of mineralized tissues (review),'' *J. Biomed. Opt.* **5**, 259–268 (2000).
3. I. C. Clarke, G. Pezzotti, S. Sakakura, and B. Ben-Nissan, ''Biolubrication phenomena affect residual stresses and phases of zirconia implants,'' *Key Eng. Mater.* **240–242**, 781–784 (2003).
4. A. Atkinson and S. C. Jain, ''Spatially resolved stress analysis using Raman spectroscopy,'' *J. Raman Spectrosc.* **30**, 885–891 (1999).
5. B. Dietrich and K. F. Dombrowski, ''Experimental challenges of stress measurements with resonant micro-Raman spectroscopy,'' *J. Raman Spectrosc.* **30**, 893–897 (1999).
6. G. Pezzotti, ''Introducing a unique measurement for biomaterial nanomechanics,'' *Key Eng. Mater.* **240–242**, 893–900 (2003).
7. I. C. Clarke, G. Pezzotti, S. Sakakura, and N. Sugano, ''Phase transformation and residual stresses in retrieved zirconia ball implant,'' *Key Eng. Mater.* **240–242**, 777–780 (2003).
8. I. C. Clarke, M. Manaka, D. D. Green, P. Williams, G. Pezzotti, Y.-H. Kim, M. Ries, N. Sugano, L. Sedel, C. Delaunay, and B. Ben-Nissan, ''Current status of zirconia used in total hip implants—clinical and laboratory studies,'' *J. Bone Jt. Surg. Am.* **85**-A (Suppl. 4) 73–84 (2003).
9. K. Haraguchi, N. Sugano, T. Nishii, H. Miki, K. Oka, and H. Yoshikawa, ''Phase transformation of a zirconia ceramic head after total hip arthroplasty,'' *J. Bone Jt. Surg. Br.* **83-B**, 996–1000 (2001).
10. X. Zhao and D. Vanderbilt, ''Phonons and lattice dielectric properties of zirconia,'' *Phys. Rev. B* **65**, 075105-1-10 (2002).
11. T. Shimanouchi and M. Tsuboi, ''Optically active lattice vibrations as treated by the GF-matrix method,'' *J. Chem. Phys.* **35**, 1597–1612 (1961).
12. B. Basu, R. G. Vitchev, J. Vleugels, J. P. Celis, and O. Van der Biest, ''Influence of humidity on the fretting wear of self-mated tetragonal zirconia ceramics,'' *Acta Mater.* **48**, 2461–2471 (2000).
13. D. R. Clarke and F. Adar, ''Measurement of the crystallographically transformed zone produced by fracture in ceramics containing tetragonal zirconia,'' *J. Am. Ceram. Soc.* **65**, 284–288 (1982).
14. V. Sergo, D. R. Clarke, and W. Pompe, ''Deformation bands in ceria-stabilized tetragonal zirconia/alumina: I, Measurement of internal stresses,'' *J. Am. Ceram. Soc.* **78**, 633-640 (1995).